



Monitoring and assimilation tests with TROPOMI data in the CAMS system. Part 1: Near-real time total column ozone

Antje Inness¹, Johannes Flemming¹, Klaus-Peter Heue², Christophe Lerot³, Diego Loyola², Roberto Ribas¹, Pieter Valks², Michel van Roozendaal³, Jian Xu² and Walter Zimmer²

5 ¹ECMWF, Shinfield Park, Reading, RG2 9AU, UK

²German Aerospace Centre (DLR), Remote Sensing Technology Institute, Oberpfaffenhofen, 82234 Wessling, Germany

³BIRA-IASB, Brussels, Belgium

10 *Correspondence to:* Antje Inness (a.inness@ecmwf.int)

Abstract

The TROPospheric Monitoring Instrument (TROPOMI) on board the Sentinel 5 Precursor (S5P) satellite launched in October 2017 yields a wealth of atmospheric composition data, including retrievals of total column ozone (TCO₃) that are provided in
15 near-real time (NRT) and off-line. These NRT TCO₃ retrievals (V1.0.0) have been included in the data assimilation system of the Copernicus Atmosphere Monitoring Service (CAMS), and tests to monitor the data and to carry out first assimilation experiments with them have been performed for the period 26 November 2017 to 3 May 2018. TROPOMI was still in its commissioning phase until 24 April 2018. Nevertheless, the results show that, even at this early stage, the TROPOMI TCO₃ data generally agree well with the CAMS analysis over large parts of the Globe and also with TCO₃ retrievals from the Ozone
20 Monitoring Instrument (OMI) and the Global Ozone Monitoring Experiment-2 (GOME-2) that are routinely assimilated by CAMS. However, the TCO₃ NRT data from TROPOMI show some retrieval anomalies at high latitudes, at low solar elevations and over snow/ice (e.g. Antarctica) where the differences with the CAMS analysis and the other datasets are larger. These differences come mainly from the surface albedo climatology that is used in the NRT TROPOMI TCO₃ retrieval. This climatology has a coarser horizontal resolution than the TROPOMI TCO₃ data which leads to problems in areas where there
25 are large changes in reflectivity from pixel to pixel, e.g. pixels covered by snow/ice or not.

The assimilation of TROPOMI TCO₃ has been tested in the CAMS system for data between 60°N and 60°S and for solar elevations less than 10° and is found to have only little impact on the ozone analysis, because the CAMS analysis is already well constrained by several other ozone retrievals that are routinely assimilated. Variational bias correction is applied to the
30 TROPOMI NRT TCO₃ data and successfully corrects for the biases seen in the data. Averaged over the period 26 November 2017 to 3 May 2018, difference between experiments with and without assimilation of TROPOMI data are less than 2% for TCO₃ and less than 1% in the vertical for averaged zonal mean O₃ mixing ratios. Compared to independent observation (Brewer spectrometers, ozone sondes, IAGOS ozone profiles and GAW surface measurements) the differences between the assimilation run and a run without TROPOMI assimilation are also small. The only noteworthy differences between the
35 experiment with and without assimilation of TROPOMI data are seen compared to IAGOS profiles at West African airports where the assimilation of TROPOMI improves the fit of the CAMS analysis to the independent data.

Despite the small impact of TROPOMI TCO₃ in the CAMS analysis it will be beneficial to include the TROPOMI TCO₃ NRT data actively in the operational NRT CAMS analysis after more tests. This will add some redundancy and resilience in
40 the system and will allow us to use a more robust observation system in case some of the other older instruments, whose retrievals are currently assimilated by CAMS, stop working.



1 Introduction

The Copernicus Atmosphere Monitoring Service (CAMS, atmosphere.copernicus.eu) produces daily global near-real time (NRT) forecasts of atmospheric composition up to five days ahead and a range of other datasets on global and regional atmospheric composition, such as near-real-time estimates of fire emissions, reanalyses of atmospheric composition and greenhouse gas forecasts and analyses. To improve the quality of the global CAMS forecasts the initial conditions for some of the chemical species, including ozone (O₃), carbon monoxide (CO), nitrogen dioxide (NO₂), sulphur dioxide (SO₂) and for aerosols are improved by assimilating satellite retrievals of atmospheric composition using a 4-dimensional variations (4D-Var) data assimilation system (Benedetti et al., 2009; Inness et al., 2013; Massart et al., 2014, Inness et al., 2015) of the European Centre for Medium Range Weather Forecasts (ECMWF).

10

A wealth of new atmospheric composition data has become available with the launch of the Sentinel 5-Precursor (S5P) satellite in October 2017. S5P carries the TROPOspheric Monitoring Instrument (TROPOMI) which provides high resolution spectral measurements in the ultraviolet (UV), visible (VIS), near infrared (NIR) and shortwave-infrared (SWIR) part of the spectrum. This wide spectral range allows several atmospheric trace gases to be retrieved, e.g. O₃, NO₂, SO₂ and HCHO from the UVVIS, and CO and CH₄ from the SWIR part of the spectrum. These species are all included in the CAMS system, making TROPOMI the perfect instrument to provide observations for the CAMS NRT analysis at unprecedented horizontal resolution of about 3.5 km x 7 km for the TROPOMI UVVIS and 7 km x 7 km for the SWIR products. In this paper, we evaluate TROPOMI near-real-time total column ozone (TCO3) retrievals (V1.0.0) produced by the Deutsche Zentrum für Luft- und Raumfahrt (DLR) against the CAMS ozone analysis for the period 26 November 2017 to 3 May 2018 and carry out first assimilation tests with the TROPOMI TCO3 data in the CAMS system. The satellite was still in its so-called commissioning phase until 24 April 2018 which is mainly used for functional testing, in-flight calibration and testing of processing chains. Nevertheless, observations were available in these early months and allowed us to prepare the CAMS system for the new data and to carry out some first tests.

15

20

Ozone plays an important role in tropospheric chemistry. Tropospheric ozone is a regional scale pollutant and, at high concentrations near the surface, harmful to humans and vegetation. Photolysis of ozone, followed by reaction with water vapour, provides the primary source of the hydroxyl radical. Ozone is also a significant greenhouse gas, particularly in the upper troposphere (Hansen et al. 1997). Tropospheric ozone is formed when Nitrogen Oxides (NO_x), CO, and Volatile Organic Compounds (VOCs) react in the presence of sunlight. In urban areas in the northern hemisphere (NH) high ozone levels usually occur during spring and summer. About 90% of the total ozone amount resides in the stratosphere, a result of oxygen photolysis as first explained by Chapman (Chapman, 1930). This ozone layer absorbs a large part of the sun's harmful UV radiation. Anthropogenic chlorofluorocarbons led to a global decrease of the ozone total column, with potentially catastrophic consequences avoided thanks to the Montreal Protocol (Newman et al., 2009). Over Antarctica, ozone destruction during Austral spring still leads to strong and rapid depletion of the ozone layer ("ozone hole"). There is evidence that the ozone hole is slowly recovering (Strahan and Douglass, 2018; Weber et al., 2018) and predictions suggest it should return to pre-1980s levels by the 2060s (Newman et al. 2006). Stratospheric ozone destruction also happens on a smaller scale over the Arctic in boreal spring (Manney et al., 2011) while ozone downward trends in the mid-low latitude lower stratosphere are related to atmospheric dynamics (Chipperfield et al., 2018).

30

35

Ozone interacts with radiation and is therefore an important parameter in radiation schemes used in Numerical Weather Prediction (NWP) models (e.g. Hogan et al., 2017), where an improved representation of the ozone field can lead to improvements in weather forecasting or climate simulations. Ozone and the assimilation of ozone retrievals was therefore included in ECMWF's Integrated Forecast System (IFS) system in the late 1990s (Hólm et al., 1999) and a stratospheric ozone

40



parameterization based on Cariolle and Teyssèdre (2007) is still used in the operational ECMWF NWP system where ozone retrievals and ozone sensitive radiances are assimilated (Dethof and Hólm, 2004; Dragani and McNally, 2011; Dragani, 2013). Because this stratospheric ozone parameterisation does not provide realistic tropospheric ozone fields, a comprehensive tropospheric chemistry scheme is used in the CAMS system (Flemming et al., 2015; Flemming et al., 2017).

5

It is hoped that by adding the assimilation of TROPOMI TCO₃ NRT data in the CAMS system, CAMS ozone analyses and forecasts will be improved and that resilience is added in the system against the loss of any of the older instruments whose O₃ retrievals are currently assimilated by CAMS (see Table 1 below). In a first step, the TROPOMI TCO₃ data are monitored passively with the CAMS system. This means they are included in the CAMS data assimilation system, the model fields are interpolated in time and space to the location of the observations and the model equivalents of the observations are calculated (e.g. by calculating vertical integrals or by applying the averaging kernels of the data to the model fields) allowing temporal and spatial statistics of the differences between the observations and collocated model fields to be calculated. However, the data are not actively used in the assimilation and do not influence the analysis and subsequent forecast yet. We call this ‘monitoring’ of the observations. In a second step, the active assimilation of the TROPOMI TCO₃ data is tested and their impact on the CAMS ozone analysis is assessed by looking at independent validation data.

10
15

The differences between the observations and the model fields are called departures. We distinguish between first-guess departures (observations minus model first-guess field) and analysis departures (observations minus analysed field). The first-guess field is a forecast initialised from the previous analysis cycle that is not changed by the analysis increments of the current analysis cycle. If the model fields are stable the departures normally show a relatively smooth behaviour from day to day. Long term monitoring of the departures can disclose errors and biases in the satellite data products, as well as errors or biases in the model. Because the departures are usually small they show up changes more clearly than when looking at the absolute model fields or observation values. A sudden jump in the departures on a global scale, which is larger than the instrument noise, can be an indication of problems in the observations or the model.

20
25

Including TROPOMI TCO₃ data passively in the CAMS system enables us to carry out a continuous quality assessment of the data, to detect biases between different satellite retrievals (e.g. between TCO₃ from TROPOMI and the Ozone Monitoring Instrument (OMI) or the Global Ozone Monitoring Experiment-2 (GOME-2)) and allows us to monitor instrument and algorithm stability. The advantage of using an assimilation system to monitor satellite data is that it provides continuous global coverage and allows us to build up global and regional statistics quickly. If the monitoring shows the data to be of good quality, i.e. departures are stable, there are no sudden jumps, the biases with respect to the model are not too large, assimilation tests with the data usually follow.

30

This paper is structured in the following way. Section 2 describes the CAMS model and data assimilation system as well as the TROPOMI TCO₃ NRT retrievals and how they are used in the CAMS system. Section 3 shows results of monitoring experiments with the TROPOMI TCO₃ data, results from first assimilation tests with the data and the validation of the resulting ozone analyses with independent observations. Section 4 gives the conclusions.

35



2 Model and Observations

2.1 CAMS model and data assimilation system

The chemical mechanism of the IFS is an extended version of the Carbon Bond Mechanism 5 (CB05, Huijnen et al. 2010) as implemented in Chemical Transport Model (CTM) Transport Model 5 (TM5) and is documented in Flemming et al. (2015) and Flemming et al. (2017). This is a tropospheric chemistry scheme, and for stratospheric ozone the chemical tendencies above the tropopause are computed by a parameterisation based on Cariolle and Teysse re (2007). The spatial resolution of the model is approximately 40 km (T511 spectral and 0.35° by 0.35° grid), i.e. coarser than the 3.5 km x 7 km resolution of the TROPOMI TCO3 data.

10 The CAMS system uses MACCity anthropogenic emissions (Granier et al., 2011), biomass burning emissions from the Global Fire Assimilation System (GFAS, Kaiser et al., 2012) and biogenic emissions from the MEGAN model (Guenther et al., 2006).

ECMWF's IFS uses an incremental 4D-Var data assimilation system going back to Courtier et al. (1994). The data assimilation system for the atmospheric composition fields remains unchanged to the one described in Inness et al. (2015). The atmospheric composition fields are included in the control vector and minimized together with the meteorological control variables. The CAMS NRT system uses 12-hour assimilation windows from 03 UTC to 15 UTC and 15 UTC to 03 UTC and two minimisations at spectral truncations T95 (~ 210 km) and T159 (~ 110 km).

Several ozone retrievals are assimilated in the CAMS NRT system (see Table 1). These include TCO3 retrievals from OMI on the Aura satellite and GOME-2 on Meteorological Operational satellite programme (Metop)-A and -B satellites (referred to as GOME-2AB), O₃ profile data from the Microwave Limb Sounder (MLS) and O₃ partial columns from Solar Backscatter Ultra-Violet (SBUV/2) and from the Ozone Mapping and Profiler Suite (OMPS). The GOME-2 and OMI TCO3 retrievals are thinned to a horizontal resolution of 0.5° x 0.5° by randomly selecting an observation in a grid box. The MLS profiles and partial column SBUV/2 and OMPS data are used unthinned at present.

25 The O₃ retrievals assimilated in the CAMS system are total or partial column data, i.e. integrated layers bounded by a top and a bottom pressure. The model's background column value is calculated as a simple vertical integral between the top and the bottom pressure of the partial or total columns, at the time and location of the observations. Averaging kernels are currently not used for the assimilation of ozone retrievals in the CAMS system, because they were either not available with the data or because the use of height resolved profile data such as MLS made their use unnecessary. Furthermore, the use of averaging kernels for stratospheric trace gas columns is not as important as for tropospheric/boundary layer trace gases (such as tropospheric NO₂). However, the use of averaging kernels for the ozone assimilation will be tested in future.

A variational bias correction (VarBC) scheme (Dee and Uppala, 2009) where biases are estimated during the analysis by including bias parameters in the control vector was used for several of the O₃ retrievals. In this scheme, the bias corrections are continuously adjusted to optimize the consistency with all information used in the analysis. VarBC is applied to the TCO3 retrievals from OMI and GOME-2 and to the partial column OMPS data, with solar elevation and a global constant as predictors, while the partial column SBUV/2 and the profile MLS data are used to anchor the bias correction, i.e. are assimilated without correction. Experience from past experiments had shown that it is important to have an anchor for the O₃ bias correction, to avoid drifts in the O₃ fields (Inness et al., 2013).



Variational quality control (Andersson and Järvinen, 1999) and first-guess quality checks are applied to all O₃ data in the CAMS system. The variational quality control reduces the weight given to observations in the analysis if they have large background departures. In the first-guess quality check, observations are rejected if the square of the normalized background departure exceeds its expected variance by more than a predefined multiple (5 for most variables).

5

2.2 TROPOMI TCO₃ NRT retrievals

TROPOMI has a local overpass time of 13:30 UTC, a ground pixel size of 3.5 km x 7 km for TCO₃ and other gases retrieved from the UVVIS, a swath of 2600 km and provides daily global coverage with ~14 orbits per day. For the work in this paper we use TROPOMI TCO₃ data (V1.0.0) that were reprocessed with the NRT algorithm (Loyola et al., 2019) for the period 26
10 November 2017 to 3 May 2018.

The TROPOMI TCO₃ retrieval is based on the GDP 4.x algorithm original developed for GOME (van Roozendaal et al., 2006), adapted to SCIAMACHY (Lerot et al., 2009) and further improved for GOME-2 (Loyola et al., 2011; Hao et al., 2014). The major TCO₃ algorithm updates for TROPOMI are the more precise treatment of clouds as scattering layers (Loyola et al.,
15 2018), an optimized wavelength for the calculation of air mass factors, better a-priori ozone profile information and a destriping correction.

We use the following quality checks to remove any outliers of the TROPOMI TCO₃ data. Data are only used if:

1. Value of quality flag given in the data ('qa flag') between [0, 100]
- 20 2. Ozone values between [0,900 DU]
3. Surface altitude between [-399, 8850m]
4. Cloud Fraction between [0,1]

Data that pass the above four checks are flagged as 'good' and used for the studies presented in this paper. In the current TROPOMI TCO₃ products V1.1.x (Pedernana et al., 2018) the 'qa flag' will allow the user to identify good quality data, but
25 this was not yet the case in V1.0.0.

Because the horizontal resolution data of TROPOMI (3.5 km x 7 km) is higher than the model resolution of T511 (about 40 km x 40 km) the TROPOMI data are not spatially representative for the model grid boxes. To overcome this representativeness error, the data are converted to so called 'super-observations' before they are included in the CAMS system. For this super-
30 obbing the data are averaged to the T511 resolution of the model. The averaging is carried out for all 'good' data and the errors of the data are averaged in the same way as the observations. The super-obbing reduces the random errors in the data. In the past a 'random' thinning to 0.5°x0.5° was used in the CAMS system and this is still applied to the TCO₃ retrievals from GOME-2 and OMI. The super-obbing applied to TROPOMI data has the advantage that it does not simply throw out the majority of the observations but uses the information from all good data to create average observations. In future, super-obbing
35 will also be tested for the other ozone datasets. An example of TROPOMI TCO₃ NRT data at full resolution and super-obbed to T511 is shown in Figure 1. The super-obbing reduces the number of 'good' TROPOMI TCO₃ data from about 15-16 million per day to about 500,000 while still making use of the information given by all good data.



3 Results

Two experiments were run with NRT TROPOMI TCO₃ data (V1.0.0) super-obbed to T511 horizontal resolution. In the first control experiment (CTRL) the TROPOMI data were included passively, in the second one (ASSIM) the data were actively assimilated between 60°N and 60°S, at solar elevations greater than 10° and if they passed the quality checks described in Section 2.2. The experiments cover the period from 26 November 2017 to 3 May 2018 and were run in hindcast mode using CY45R1 of the CAMS system.

3.1 Monitoring of TROPOMI TCO₃ NRT data

Figure 2 shows the mean TCO₃ fields averaged over the period from 26 November 2017 to 3 May 2018 from TROPOMI and the other three TCO₃ retrievals that are routinely assimilated in the CAMS NRT system, i.e. OMI and GOME-2AB. For TROPOMI ‘good’ data (see Section 2.2) super-obbed to T511 are shown, while for the other three instruments ‘used’ data are shown, i.e. the data that passed all quality and blacklist checks (see Table 1) and were actively assimilated. Figure 2 shows that all four instruments agree well and TROPOMI successfully captures the structures of the global ozone field with high values in the NH Extratropics, low values in the Tropics and higher values in a band surrounding Antarctica.

Figure 3 shows difference plots of TROPOMI and the other retrievals and illustrates that there are pronounced differences between the data sets that show up less clearly when looking at the absolute fields in Fig. 2. TROPOMI is higher than the other three retrievals in the NH south of 60°N, with positive differences of up to 60 DU in places between about 40–60°N. Poleward of that, TROPOMI is mainly lower than GOME-2AB while there are positive and negative differences compared to OMI. In the southern hemisphere (SH), the differences are smaller and mainly negative between 0–60°S, but larger negative differences are found over Antarctica. Because the differences show similar structures over Antarctica for OMI and GOME-2AB they are likely to point to problems with the TROPOMI retrievals rather than the other datasets.

Figure 4 shows maps of the standard deviation of the four TCO₃ retrievals over the period from 26 November 2017 to 3 May 2018. All retrievals show the same features with highest variability in the northern Extratropics and lowest variability in the Tropics.

Figure 5 shows mean analysis departures from the four TCO₃ retrievals. Because the GOME-2AB and OMI retrievals are actively assimilated in the CAMS system and the analysis is drawing to the data their analysis departures are generally smaller than TROPOMI’s. OMI has larger analysis departures than GOME-2AB with negative departures in the high Arctic and positive departures over the Tropics and over sea south of about 60°S. This might point to a problem with the OMI retrievals, which is not completely removed by the bias correction during the analysis. TROPOMI shows larger analysis departures than the other three retrievals, partly because the data are not being assimilated, but also because of issues with the TROPOMI NRT TCO₃ retrievals. These problems show up better in the departure plots than in the plot of absolute values (Fig. 2). TROPOMI is lower than the CAMS analysis south of 60°S and over land or snow/ice north of 60°N. TROPOMI is considerably higher than the CAMS analysis over land in the NH north of about 40°N. These differences come mainly from the surface albedo climatology that is used in the TROPOMI NRT retrieval algorithm of the V1.0.0 data. The employed surface albedo climatology, based on OMI data (Kleipool et al., 2008), has a spatial resolution of 0.5° x 0.5° which seems coarser than the spatial resolution of the TROPOMI pixels. Consequently, surface albedo structures are found in the obtained TCO₃ results, particularly over the polar regions where the surface albedo climatology sometimes has very few grid cells marked as no snow or ice (reflectivity 0.05) whereas the reflectivity is close to one for the neighbouring ones with snow. In the near future, it is planned to replace this coarse climatology with a new albedo climatology based on S5P data. Large positive TROPOMI TCO₃ departures are also seen over the Himalayas. In the other areas, TROPOMI agrees better with the model, with positive



departures over the tropical Atlantic, Africa and South America (similar to OMI) and small negative departures elsewhere. Figure 5 illustrates the power of using a global assimilation system to monitor new data sets, as it gives a global picture and builds up statistics quickly.

5 The positive departures north of 40°N can also be seen in histograms of departures (Fig. 6) which show a positive mean bias with respect to CAMS of 0.35 ± 12.8 DU in the NH with a tail of large positive departures, a mean value of 0.69 ± 3.54 DU in the Tropics and a negative mean value of -2.83 ± 7.42 DU in the SH with a long tail of negative departures. The mean bias in the NH is small because the positive bias south of about 60°N and the negative one north of 60°N compensate. This is illustrated by the large standard deviation in the NH. Table 2 lists the mean biases and standard deviations from all four TCO3 retrievals
10 and shows that the biases of TROPOMI are of similar magnitude to the biases of the other instruments. The standard deviation of the TROPOMI departures is larger than GOME-2AB's, but smaller than OMI's in the NH and similar to OMI's in the Tropics.

Figure 7 shows timeseries of daily mean area averaged TROPOMI TCO3 departures, observation and analysis values as well
15 as the number of observations from 26 November 2017 to 3 May 2018 for the NH, the Tropics and SH. The Figure shows that there are long periods without TROPOMI data in December 2017 and January 2018 when the instrument was undergoing calibration activities and a shorter period without data at the beginning of March 2018. The S5P satellite was still in its commissioning phase until 24 April 2018 which led to interruptions of the data availability. From mid-February onwards the number of data is more stable and the departures are smoother. The departures are positive in the NH and Tropics and negative
20 in the SH. In the NH, the TROPOMI analysis departures are actually larger than the first-guess departures from mid-February onwards, showing that the assimilation of GOME-2AB and OMI adds information to the analysis that is contrary to the TROPOMI data. In the Tropics, the TROPOMI analysis departures are generally smaller than the first-guess departures illustrating that the data are more consistent with the other O₃ data used in the analysis as the assimilation of the other data improves the fit of the analysis to the (not assimilated) TROPOMI data. In the SH, the TROPOMI first-guess and analysis
25 departures are similar. Comparing the magnitude of the departures with the observation and analysis values shows that in relative terms the area averaged TROPOMI departures are small. They are less than 1% in the NH and SH and less than 0.5% in the Tropics.

Figure 8 shows a timeseries of zonal mean daily analysis departures from TROPOMI and illustrates that the evolution of the
30 departures with time is quite stable between about 60°S–60°N where departures are small, but that there are larger variations (and larger departures) at the northern and southern ends of the orbits. Similar features are also seen for TCO3 from OMI and GOME-2AB (not shown).

Figure 9 shows scatter plots of TROPOMI TCO3 analysis departures for the period 26 November 2017 to 3 May 2018 against
35 latitude, solar elevation, cloud cover, cloud top pressure and scan position. Such plots can be very useful in identifying retrieval problems depending on the chosen parameters. The scatter plot against latitude shows small mean departures between about 60°S and 50°N, positive departures between 40°N and 70°N and negative departures poleward of 70°N and 60°S. This is in agreement with the averaged analysis departures shown in Fig. 5 and the Hovmoeller plot in Fig. 8 and illustrates that there is a problem with the retrievals at high latitudes. The plot also shows that there is a large scatter polewards of 50°N and 60°S.
40 Larger scatter at high latitudes is also seen for OMI and GOME-2AB if all 'good' data are plotted (not shown). Furthermore, the TROPOMI departures show a dependency on solar elevation with small or slightly positive departures for solar elevations greater than about 25° and increasingly negative departures at lower solar elevations. There is no obvious dependency of the departures on cloud cover or cloud top pressure, but the departures vary slightly depending on the scan position with



increasingly negative departures towards the edges of the scan, especially on the left side of the scan. This dependency indicates possible limitations of the TROPOMI TCO₃ NRT destriping correction.

3.2 Assimilation tests with TROPOMI TCO₃ NRT data

5 We showed in section 3.1 that the TROPOMI TCO₃ data are of good quality over large parts of the globe, but that there are issues at high latitudes and low solar elevations. The biases we observe outside those regions are of similar magnitude to the biases of the other total column data sets assimilated in CAMS (see Table 2) and we therefore do not expect any problems with the assimilation of TROPOMI NRT TCO₃ if we bias correct the data and blacklist them appropriately. Hence, assimilation tests are carried out with the TROPOMI NRT TCO₃ data (V1.0.0) for the period 26 November 2017 to 3 May 2018,
10 blacklisting them for solar elevations less than 10° and poleward of 60°. Variational bias correction is applied to the data in the same way as it is used for the other TCO₃ data, i.e. with solar elevation and a global constant as predictors.

3.2.1 Impact of the TROPOMI assimilation

Figure 10 shows timeseries of daily global mean TROPOMI, OMI and GOME-2AB TCO₃ departures, standard deviation of departures and number of observations between 26 November 2017 and 3 May 2018 for ‘used data’, i.e. the data that fulfil the
15 quality check listed in Table 1 and pass the variational quality control and first-guess checks applied by the IFS (see section 2.1). The figure shows that the TROPOMI bias correction successfully removes the bias between the data and the model, so that the bias corrected analysis departures and their standard deviations are small. The bias correction has values of about 0.5 DU in the global mean after March and smaller or small negative values before then. The magnitude of the global mean bias correction that is applied to TROPOMI is smaller than that of the other three TCO₃ retrievals. The figure shows that the
20 analysis is drawing to the TROPOMI data and analysis departures are smaller than the first-guess departures and the standard deviation of the departures is reduced. We also see how many more data are used from TROPOMI than from OMI, GOME-2A and GOME-2B: about 360,000 per day compared to 36,000, 75,000 and 110,0000 respectively.

Table 3 lists mean biases and standard deviations for all four TCO₃ retrievals for the period 26 November 2017 to 3 May 2018
25 from ASSIM. It shows that TROPOMI TCO₃ bias and standard deviation values are reduced in all three areas compared to the values in CTRL (see Table 2) as the analysis is drawing to the data. In the Tropics, the bias and standard deviation of OMI and GOME-2AB are also smaller in ASSIM than in CTRL because of the additional constraint from the TROPOMI assimilation. The fit to OMI and GOME-2A TCO₃ is degraded in the NH and SH in ASSIM, but for GOME-2B it is improved in all areas. The size of the TROPOMI biases in Table 3 is similar to GOME-2AB’s and smaller than OMI’s.

30

Figure 11 shows that the mean bias-corrected TROPOMI analysis departures for the period 26 November to 3 May 2018 are small (compared to Fig.5) because the analysis is drawing to the data. Some larger positive departures remain over land in the NH where observation outliers are given less weight by the analysis. The figure also shows that the mean bias correction for TROPOMI is positive at high latitudes and negative in the Tropics and that it changes with time to adjust to the changes in the
35 data.

Figure 12 shows the mean TCO₃ fields from ASSIM and CTRL as well as their absolute and relative differences averaged over the period 26 November 2017 to 3 May 2018. It illustrates that the impact of the TROPOMI assimilation (both in absolute and relative terms) is small. Absolute differences are less than 1 DU over most of the Globe with maximum differences of less
40 than 2 DU around 50°N and over Africa, where ASSIM has larger TCO₃ values than CTRL. In relative terms, the differences



are less than 2% everywhere (and less than 1% in most areas) with negative relative differences between 20-50°S, 20-40°N and over the Pacific between 50°S and 40°N. Positive differences are seen over Africa and over land between about 40-60°N.

Figure 13 shows a cross section of zonal mean relative O₃ mixing ratio differences from ASSIM minus CTRL averaged over the period 26 November 2017 to 3 May. Again, the impact of TROPOMI assimilation is small and differences between ASSIM and CTRL are less than 1% everywhere. The largest relative differences are seen in the troposphere.

The impact of the TROPOMI assimilation in the CAMS system is so small because the CAMS analysis is already well constrained by the other data sets that are assimilated routinely (see Table 1). If no other O₃ data were available and only TROPOMI TCO₃ data were assimilated the impact on the CAMS O₃ analysis would be larger.

3.2.2 Validation with independent observations

To assess if the assimilation of TROPOMI TCO₃ retrievals improves or degrades the CAMS analysis, the O₃ fields from ASSIM and CTRL are compared with independent observations. We use for comparison the following datasets. (1) Brewer spectrometer measurements obtained from the World Ozone and Ultraviolet Radiation Data Centre (WOUDC). The Brewer data are well calibrated with a precision of 1% (Basher, 1982). (2) Ozone sonde data from a variety of data centres: WOUDC, Southern Hemisphere ADDitional OZonesondes (SHADOZ), Network for the Detection of Atmospheric Composition Change (NDACC), and campaigns for the Determination of Stratospheric Polar Ozone Losses (MATCH). The precision of electrochemical concentration cell (ECC) ozone sondes is on the order of ±5% in the range between 200 and 10 hPa, between -14% and +6% above 10 hPa, and between -7% and +17% below 200 hPa (Komhyr et al., 1995). Larger errors are found in the presence of steep gradients and where the ozone amount is low. The same order of precision was found by Steinbrecht et al. (1998) for Brewer–Mast sondes. (3) Ozone profiles from instruments mounted on commercial aircraft from the In-service Aircraft for a Global Observing System (IAGOS). The IAGOS ozone data have a detection limit of 2 ppbv and a precision of ± (2 ppbv + 2 %) (Marengo et al., 1998). (4) Ground-based data from the World Meteorological Organisation's Global Atmosphere Watch (GAW) surface observation network (e.g., Oltmans and Levy, 1994; Novelli and Masarie, 2014). The GAW observations represent the global background away from the main polluted areas. GAW O₃ data have a precision of ±1 ppbv (Novelli and Masarie; 2014).

Figure 14 shows timeseries of the daily TCO₃ biases from ASSIM and CTRL against Brewer measurements averaged over the Globe and Europe and confirms that the impact of the TROPOMI assimilation in the CAMS system is small, because there are no significant differences between ASSIM and CTRL (as already seen in Fig. 12 and 13). Compared with ozone sondes (Fig. 15) and IAGOS O₃ profiles (Fig. 16) the impact is also small. The largest impact is found over the West African airports (Fig. 16) where the negative bias of CAMS is reduced in ASSIM throughout the troposphere. Here the increased O₃ values seen in Fig. 12 and Fig. 13 lead to an improved fit with the aircraft data. Finally, we compare ASSIM and CTRL with GAW O₃ surface observation in Figure 17 and again see hardly any impact from the TROPOMI assimilation.

4 Conclusions

TROPOMI NRT TCO₃ retrievals have been included in the CAMS data assimilation system to first monitor the data and then carry out assimilation tests with them. The TROPOMI data used for the work presented in this paper were TROPOMI TCO₃ data (V1.0.0) that had been reprocessed with the NRT algorithm (Loyola et al., 2019) for the period 26 November 2017 to 3 May 2018. TROPOMI was still in its commissioning phase until 24 April 2018, but even at this early stage the TROPOMI



TCO3 data generally agreed well with the CAMS analysis over large parts of the Globe and were of good enough quality to test their use in the CAMS system.

Monitoring of TROPOMI TCO3 data in the CAMS system has shown that the data are of good quality over large parts of the
5 Globe where the biases they have relative to the CAMS O₃ analysis are of similar magnitude to biases of OMI and GOME-2AB TCO3. However, there are problems with the TROPOMI TCO3 NRT retrievals at high latitudes, at low solar elevations and over snow/ice (e.g. Antarctica). These differences come mainly from the surface albedo climatology that is used in the TROPOMI NRT retrieval algorithm of the V1.0.0 data and has a spatial resolution of 0.5° x 0.5° which is coarser than the spatial resolution of the TROPOMI pixels. The bias of TROPOMI TCO3 relative to CAMS also depends slightly on scan
10 position, with increasingly negative bias towards the edges of the scan. This shows limitations of the current destriping algorithm.

Relative to CAMS and averaged over the period 26 November 2017 to 3 May 2018, TROPOMI TCO3 NRT data show a mean bias of 0.35±12.8 DU in the NH, a mean bias of 0.69±3.54 DU in the Tropics and a mean bias of -2.83±7.42 DU in the SH.
15 The small mean bias in the NH is the result of compensating positive and negative biases as indicated by the large standard deviation. These biases are of similar magnitude to the biases of the other TCO3 datasets (OMI, GOME-2AB) assimilated in the CAMS system, though TROPOMI NRT TCO3 is up to 60 DU higher in NH mid-latitudes in places (Figure 3).

Assimilation tests were carried out with the TROPOMI TCO3 data, blacklisting them poleward of 60° and at solar elevations
20 less than 10°, and applying ECMWF's variational bias correction scheme to the data with solar elevation and a global constant as predictors. These assimilation tests showed that the bias correction successfully removed the biases between the model and the data. On the whole, the impact of the TROPOMI data in the CAMS assimilation system was found to be small, because the ozone analysis is already well constrained by all the other ozone data sets that are assimilated routinely (OMI, GOME-2AB, MLS, SBUV/2, OMPS). Mean differences between a run with and without assimilation of TROPOMI TCO3 NRT data
25 over the period 26 November 2017 to 3 May 2018 are less than 2% for TCO3 and less than 1% in the vertical for average zonal mean O₃ mixing ratios. The two runs showed hardly any differences when compared with independent ozone observations, the largest noticeable impact of the TROPOMI assimilation was found over West African airports, where the assimilation led to increased ozone values in the troposphere and a slightly reduced negative bias against IAGOS aircraft profiles.

30 However, the tests also illustrate that the assimilation of TROPOMI data in the CAMS system does not degrade the ozone analysis, suggesting it should be straight forward to activate the TROPOMI assimilation in the operational NRT CAMS analysis. It would indeed be beneficial to include the TROPOMI TCO3 NRT data actively in the operational NRT CAMS analysis soon, despite the small impact, to add redundancy and resilience and to have a more robust observation system in
35 place if some of the other older instruments, whose retrievals are currently assimilated by CAMS, stop working.

Due to the limitations of the TROPOMI TCO3 NRT V1.0.0 product, ozone data had to be blacklisted at high latitudes in this study. Future algorithm updates dealing with a better treatment of the surface albedo will improve the retrieval quality at high latitudes and should allow the data to be used up to the poles. Note that the TROPOMI TCO3 offline algorithm does not have
40 this limitation seen in the NRT product because the surface albedo is fitted as part of the retrieval.

The paper illustrates the power of using a global assimilation system to monitor new satellite products, as it provides continuous global coverage, allows us to build up global and regional statistics quickly and can help to identify problems with the retrievals



(e.g. biases against solar elevation, latitude, scan position, surface albedo dependencies, etc.) that might be more difficult to discover when comparing TROPOMI retrievals against sparse in-situ observations.

TROPOMI TCO3 NRT data were included passively in the operational CAMS NRT system on 13 July 2018, when they were
5 officially released by ESA, and have been monitored routinely by CAMS ever since (see https://atmosphere.copernicus.eu/charts/cams_monitoring). Assimilation tests with the data continue and it is expected that the assimilation of TROPOMI NRT TCO3 data in the operational CAMS analysis will begin soon.

Author Contributions

10 A. Inness carried out the experiments described in the paper, the validation of the resulting analysis fields and wrote the manuscript, R. Ribas set up the S5P processing chain at ECMWF which included coding and testing the BUFR converter needed to ingest the TROPOMI TCO3 data in the ECMWF data system, J. Flemming helped with the development of the IFS chemistry module, D. Loyola, W. Zimmer, K.-P. Heue, J. Xu, P. Valks, C. Lerot and M. van Roozendael developed the TROPOMI TCO3 retrieval algorithm and the operational processing chain at DLR. All co-authors gave useful comments
15 during the writing of the paper.

Acknowledgements

Thanks to Fabian Romahn and Mattia Pedergnana working on the operational UPAS system for generating TROPOMI TCO3 products and thanks to Maximilian Schwinger and the PDGS team at DLR responsible for the Sentinel-5 Precursor payload data ground segment. Thanks to Luke Jones for help with the plotting of ozone sondes, GAW and IAGOS data. Thanks to the
20 data providers of the data assimilated in the CAMS reanalysis and the data used for the validation studies in this paper. The GOME-2 total ozone data assimilated in CAMS are provided by DLR in the framework of the EUMETSAT AC-SAF project. The Copernicus Atmosphere Monitoring Service is operated by the European Centre for Medium-Range Weather Forecasts on behalf of the European Commission as part of the Copernicus programme (<http://copernicus.eu>).

References

- 25 Andersson, E. and Järvinen, H.: Variational quality control. *Q.J. Roy. Meteor. Soc.*, 125,697-722, 1999.
- Basher, R. E.: Review of the Dobson spectrophotometer and its accuracy, *Global Ozone Res. Monit. Proj., Rep. 13*, World Meteor. Organ., Geneva, Switzerland, December, available at: <http://www.esrl.noaa.gov/gmd/ozwv/dobson/papers/report13/report13.html> (last access: 3 February 2017), 1982.
- 30 Benedetti, A., Morcrette, J.-J., Boucher, O., Dethof, A., Engelen, R. J., Fisher, M., Flentje, H., Huneeus, N., Jones, L., Kaiser, J. W., Kinne, S., Mangold, A., Razinger, M., Simmons, A. J., Suttie, M., and the GEMS-AER team: Aerosol analysis and forecast in the European Centre for Medium-Range Weather Forecasts Integrated Forecast System: Data Assimilation. *J. Geophys. Res.*, D13205, 114, doi:10.1029/2008JD011115, 2009.
- 35 Bhartia, P. K., McPeters, R. D., Mateer, C. L., Flynn, L. E., and Wellemeyer, C., Algorithm for the estimation of vertical ozone profiles from the backscattered ultraviolet technique, *J. Geophys. Res.*, 101(D13), 18,793– 18,806, 1996.



- Cariolle, D. and Teysse re, H.: A revised linear ozone photochemistry parameterization for use in transport and general circulation models: multi-annual simulations. *Atmos. Chem. Phys.*, 7, 2183-2196, 2007.
- S. Chapman F.R.S. (1930) XXXV. On ozone and atomic oxygen in the upper atmosphere, The London, Edinburgh, and Dublin
5 *Philosophical Magazine and Journal of Science*, 10:64, 369-383, DOI: 10.1080/14786443009461588
- Chipperfield, M. P., Dhomse, S., Hossaini, R., Feng, W., Santee, M. L., Weber, M., Burrows J. P., Wild J. D., Loyola, D.,
Coldewey-Egbers M. On the cause of recent variations in lower stratospheric ozone. *Geophysical Research Letters*, 45, 5718–
5726. <https://doi.org/10.1029/2018GL078071>, 2018.
10
- Courtier, P., Th paut, J.-N. and Hollingsworth, A.: A strategy for operational implementation of 4D-Var, using an incremental
approach. *Q. J. R. Meteorol. Soc.*, 120, 1367-1388, 1994.
- Dee, D. P. and Uppala, S.: Variational bias correction of satellite radiance data in the ERA-Interim reanalysis. *Q. J. R.*
15 *Meteorol. Soc.*, 135, 1830–1841, 2009.
- Dethof, A. and H lm, E.V.: Ozone assimilation in the ERA-40 reanalysis project. *Quart. J. Roy. Met. Soc.*, 130, 2851-2872,
2004.
- 20 Dragani, R. and McNally, A. P. (2013), Operational assimilation of ozone-sensitive infrared radiances at ECMWF. *Q.J.R.*
Meteorol. Soc., 139: 2068-2080. doi:10.1002/qj.2106
- Dragani R. 2011. On the quality of the ERA-Interim ozone reanalyses: comparisons with satellite data.
Q. J. R. Meteorol. Soc. 137: 1312 – 1326. DOI:10.1002/qj.821
- 25 Flemming, J., Benedetti, A., Inness, A., Engelen, R. J., Jones, L., Huijnen, V., Remy, S., Parrington, M., Suttie, M., Bozzo,
A., Peuch, V.-H., Akritidis, D., and Katragkou, E.: The CAMS interim Reanalysis of Carbon Monoxide, Ozone and Aerosol
for 2003–2015, *Atmos. Chem. Phys.*, 17, 1945-1983, <https://doi.org/10.5194/acp-17-1945-2017>, 2017.
- Flemming, J., Huijnen, V., Arteta, J., Bechtold, P., Beljaars, A., Blechschmidt, A.-M., Diamantakis, M., Engelen, R. J., Gaudel,
30 A., Inness, A., Jones, L., Josse, B., Katragkou, E., Marecal, V., Peuch, V.-H., Richter, A., Schultz, M. G., Stein, O., and
Tsikerdekis, A.: Tropospheric chemistry in the Integrated Forecasting System of ECMWF, *Geosci. Model Dev.*, 8, 975-1003,
doi:10.5194/gmd-8-975-2015, 2015.
- Flynn, L., et al. (2014), Performance of the Ozone Mapping and Profiler Suite (OMPS) products, *J. Geophys. Res. Atmos.*,
35 119, 6181–6195, doi:10.1002/2013JD020467
- Granier, C., Bessagnet, B., Bond, T., D'Angiola, A., Denier van der Gon, H., Frost, G. J., Heil, A., Kaiser, J. W., Kinne, S.,
Klimont, Z., Kloster, S., Lamarque, J.-F., Liousse, C., Masui, T., Meleux, F., Mieville, A., Ohara, R., Raut, J.-C., Riahi, K.,
Schultz, M. G., Smith, S. G., Thompson, A., van Aardenne, J., van der Werf, G. R., and van Vuuren, D. P.: Evolution of
anthropogenic and biomass burning emissions of air pollutants at global and regional scales during the 1980-2010 period.
40 *Climatic Change*, 109, 163-190. DOI: 10.1007/s 10584-011-0154-1, 2011a.



Guenther, A., Karl, T., Harley, P., Wiedinmyer, C., Palmer, P. I., and Geron, C.: Estimates of global terrestrial isoprene emissions using MEGAN (Model of Emissions of Gases and Aerosols from Nature), *Atmos. Chem. Phys.*, 6, 3181–3210, doi:10.5194/acp-6-3181-2006, 2006.

5 Hansen, J., Sato, M., and Ruedy, R.: Radiative forcing and climate response, *J. Geophys. Res.*, 102, 6831–6864, 1997.

Hao, N., Koukouli, M. E., Inness, A., Valks, P., Loyola, D. G., Zimmer, W., Balis, D. S., Zyrichidou, I., Van Roozendael, M., Lerot, C., and Spurr, R. J. D.: GOME-2 total ozone columns from MetOp-A/MetOp-B and assimilation in the MACC system, *Atmos. Meas. Tech.*, 7, 2937–2951, <https://doi.org/10.5194/amt-7-2937-2014>, 2014.

10

Hólm, E. V., Untch, A., Simmons, A., Saunders, R., Bouvier, F., and Andersson, E. (1999). Multivariate ozone assimilation in four-dimensional data assimilation, SODA workshop on Chemical Data Assimilation, Publication 188, KNMI, De Bilt, the Netherlands.

15 Huijnen, V., Williams, J., van Weele, M., van Noije, T., Krol, M., Dentener, F., Segers, A., Houweling, S., Peters, W., de Laat, J., Boersma, F., Bergamaschi, P., van Velthoven, P., Le Sager, P., Eskes, H., Alkemade, F., Scheele, R., Nédélec, P., and Pätz, H.-W.: The global chemistry transport model TM5: description and evaluation of the tropospheric chemistry version 3.0, *Geosci. Model Dev.*, 3, 445–473, doi:10.5194/gmd-3-445-2010.

20 Inness, A., Aben, I., Agusti-Panareda, A., Borsdorff, T., Flemming, J., Landgraf, J. and Ribas, R. (2018): Monitoring and assimilation tests with TROPOMI data in the CAMS system. Part 1: Total column CO retrievals. To be submitted to ACP.

Inness, A., Blechschmidt, A.-M., Bouarar, I., Chabrilat, S., Crepulja, M., Engelen, R. J., Eskes, H., Flemming, J., Gaudel, A., Hendrick, F., Huijnen, V., Jones, L., Kapsomenakis, J., Katragkou, E., Keppens, A., Langerock, B., de Mazière, M., Melas,

25 D., Parrington, M., Peuch, V. H., Razinger, M., Richter, A., Schultz, M. G., Suttie, M., Thouret, V., Vrekoussis, M., Wagner, A., and Zerefos, C.: Data assimilation of satellite-retrieved ozone, carbon monoxide and nitrogen dioxide with ECMWF's Composition-IFS, *Atmos. Chem. Phys.*, 15, 5275–5303, doi:10.5194/acp-15-5275-2015, 2015.

Inness, A., Baier, F., Benedetti, A., Bouarar, I., Chabrilat, S., Clark, H., Clerbaux, C., Coheur, P., Engelen, R. J., Errera, Q.,

30 Flemming, J., George, M., Granier, C., Hadji-Lazarou, J., Huijnen, V., Hurtmans, D., Jones, L., Kaiser, J. W., Kapsomenakis, J., Lefever, K., Leitão, J., Razinger, M., Richter, A., Schultz, M. G., Simmons, A. J., Suttie, M., Stein, O., Thépaut, J.-N., Thouret, V., Vrekoussis, M., Zerefos, C., and the MACC team: The MACC reanalysis: an 8 yr data set of atmospheric composition, *Atmos. Chem. Phys.*, 13, 4073–4109, doi:10.5194/acp-13-4073-2013, 2013.

35 Hogan, R., and Co-authors (2017), Radiation in numerical weather prediction, ECMWF Technical Memorandum 816.

Kaiser, J. W., Heil, A., Andreae, M. O., Benedetti, A., Chubarova, N., Jones, L., Morcrette, J.-J., Razinger, M., Schultz, M. G., Suttie, M., and van der Werf, G. R.: Biomass burning emissions estimated with a global fire assimilation system based on observed fire radiative power. *Biogeosciences*, 9:527–554, 2012.

40

Kleipool, Q. L., Dobber, M. R., de Haan, J. F., and Levelt, P. F.: Earth surface reflectance climatology from 3 years of OMI data, *J. Geophys. Res.*, 113, D18308, <https://doi.org/10.1029/2008JD010290>, 2008.



- Komhyr, W. D., Barnes, R. A., Borthers, G. B., Lathrop, J. A., Kerr, J. B., and Opperman, D. P.: Electrochemical concentration cell ozonesonde performance evaluation during STOIC 1989, *J. Geo- phys. Res.*, 100, 9231–9244, 1995.
- 5 Liu, X., Bhartia, P. K., Chance, K., Froidevaux, L., Spurr, R. J. D., and Kurosu, T. P.: Validation of Ozone Monitoring Instrument (OMI) ozone profiles and stratospheric ozone columns with Microwave Limb Sounder (MLS) measurements, *Atmos. Chem. Phys.*, 10, 2539-2549, <https://doi.org/10.5194/acp-10-2539-2010>, 2010.
- Lerot, C., Van Roozendaal, M., van Geffen, J., van Gent, J., Fayt, C., Spurr, R., Lichtenberg, G., and von Bargaen, A.: Six years
10 of total ozone column measurements from SCIAMACHY nadir observations, *Atmos. Meas. Tech.*, 2, 87-98, 2009.
- Loyola, D., et al.: The near-real-time total ozone retrieval algorithm from TROPOMI onboard Sentinel-5 Precursor, *Atmos. Meas. Tech. Discuss.*, in preparation, 2019.
- 15 Loyola, D. G., Gimeno García, S., Lutz, R., Argyrouli, A., Romahn, F., Spurr, R. J. D., Pedernana, M., Doicu, A., Molina García, V., and Schüssler, O.: The operational cloud retrieval algorithms from TROPOMI on board Sentinel-5 Precursor, *Atmos. Meas. Tech.*, 11, 409-427, <https://doi.org/10.5194/amt-11-409-2018>, 2018.
- Loyola, D., M. Koukoulis, P. Valks, D. Balis, N. Hao, M. Van Roozendaal, R. Spurr, W. Zimmer, S. Kiemle, C. Lerot, and J-
20 C. Lambert, The GOME-2 Total Column Ozone Product: Retrieval Algorithm and Ground-Based Validation, *J. Geophys. Res.*, 116, D07302, doi:10.1029/2010JD014675, 2011.
- Manney, G. L. et al.: Unprecedented Arctic ozone loss in 2011. *Nature*, doi: 10.1038/nature10556, 2011.
- 25 Marengo, A., V. Thouret, P. Nédélec, H.G. Smit, M. Helten, D. Kley, F. Karcher, P. Simon, K. Law, J. Pyle, G. Poschmann, R. Von Wrede, C. Hume, and T. Cook, Measurement of ozone and water vapour by Airbus in-service aircraft: The MOZIC airborne programme, an overview, *J. Geophys. Res.*, 103, D19, 25,631-25,642, 1998.
- Massart, S., Agusti-Panareda, A., Aben, I., Butz, A., Chevallier, F., Crevoisier, C., Engelen, R., Frankenberg, C., and
30 Hasekamp, O.: Assimilation of atmospheric methane products into the MACC-II system: from SCIAMACHY to TANSO and IASI, *Atmos. Chem. Phys.*, 14, 6139-6158, <https://doi.org/10.5194/acp-14-6139-2014>, 2014.
- McPeters, R. D., P. K. Bhartia, D. Haffner, G. J. Labow, and L. Flynn (2013), The version 8.6 SBUV ozone data record: An overview, *J. Geophys. Res. Atmos.*, 118, 8032–8039, doi:10.1002/jgrd.50597.
35
- Newman, P. A., Oman, L. D., Douglass, A. R., Fleming, E. L., Frith, S. M., Hurwitz, M. M., Kawa, S. R., Jackman, C. H., Krotkov, N. A., Nash, E. R., Nielsen, J. E., Pawson, S., Stolarski, R. S., and Velders, G. J. M.: What would have happened to the ozone layer if chlorofluorocarbons (CFCs) had not been regulated?, *Atmos. Chem. Phys.*, 9, 2113-2128, doi:10.5194/acp-9-2113-2009, 2009.
40
- Newman, P. A., E. R. Nash, S. R. Kawa, S. A. Montzka, and S. M. Schauffler (2006), When will the Antarctic ozone hole recover? *Geophys. Res. Lett.*, 33, L12814, doi: 10.1029/2005GL025232.



Novelli, P.C. and Masarie, K.A.: Atmospheric Carbon Monoxide Dry Air Mole Fractions from the NOAA ESRL Carbon Cycle Cooperative Global Air Sampling Network, 1988-2013, Version: 2014-07-02, ftp://aftp.cmdl.noaa.gov/data/trace_gases/co/flask/surface/ (last access December 2014), 2014.

- 5 Oltmans, SJ and Levy II, H: Surface ozone measurements from a global network, *Atmos. Environ.*, 28, 9-24, 1994.

Pedergnana, M., et al., Sentinel-5 precursor/TROPOMI – Level 2 Product User Manual – O₃ Total Column, S5P-L2-DLR-PUM-400A available at: <https://sentinels.copernicus.eu/web/sentinel/technical-guides/sentinel-5p/products-algorithms> and <http://www.tropomi.eu/data-products/level-2-products>, 2018.

10

Schwartz, M., Froidevaux, L., Livesey, N. and Read, W. (2015), MLS/Aura Level 2 Ozone (O₃) Mixing Ratio V004, Greenbelt, MD, USA, Goddard Earth Sciences Data and Information Services Center (GES DISC), Accessed: [20180718], 10.5067/Aura/MLS/DATA2017

- 15 Strahan, S. E., & Douglass, A. R. (2018). Decline in Antarctic ozone depletion and lower stratospheric chlorine determined from Aura Microwave Limb Sounder observations. *Geophysical Research Letters*, 45, 382–390. <https://doi.org/10.1002/2017GL074830>

- 20 Steinbrecht, W., Shwartz, R., and Claude, H.: New pump correction for the Brewer-Mast ozonesonde: Determination from experiment and instrument intercomparisons, *J. Atmos. Ocean. Tech.*, 15, 144–156, 1998.

Valks, P., Loyola, D., Hao, N., Hedelt, P., Slijkhuis, S., Grossi, M., Gimeno Garcia, S., Lutz, R.: Algorithm Theoretical Basis Document - GOME-2 Total Columns of Ozone, NO₂, BrO, HCHO, SO₂, H₂O, OCLO and cloud Properties, GDP 4.8, SAF/AC/DLR/ATBD/01, Issue 3/A, 2017.

25

Van Roozendael, M., Loyola, D., Spurr, R., Balis, D., Lambert, J.-C., Livschitz, Y., Valks, P., Ruppert, T., Kenter, P., Fayt, C., and Zehner C.: Ten years of GOME/ERS-2 total ozone data: the new GOME Data Processor (GDP) Version 4: I. Algorithm Description, *J. Geophys Res.*, doi: 10.1029/2005JD006375, 2006.

- 30 Weber, M., Coldewey-Egbers, M., Fioletov, V. E., Frith, S. M., Wild, J. D., Burrows, J. P., Long, C. S., and Loyola, D.: Total ozone trends from 1979 to 2016 derived from five merged observational datasets – the emergence into ozone recovery, *Atmos. Chem. Phys.*, 18, 2097-2117, <https://doi.org/10.5194/acp-18-2097-2018>, 2018.



Instrument/ Satellite	Data product	Data provider/version	Blacklist criteria / thinning	VarBC predictors	Reference
GOME-2/ Metop-A	TCO3	AC-SAF/ DLR GDP4.8	QF>0 SOE<6° Thinned to 0.5°x0.5°	Solar elevation Global constant	Hao et al. (2014), Valks et al. (2017)
GOME-2/ Metop-B	TCO3	AC-SAF/ DLR GDP4.8	QF>0 SOE<6° Thinned to 0.5°x0.5°	Solar elevation Global constant	Hao et al. (2014), Valks et al. (2017)
MLS/ Aura	O ₃ profiles	NASA V3.4	QF>0 No thinning	Not applied	Schwartz et al. (2015)
OMI/ Aura	TCO3	NASA V883	QF>0 SOE<10° Thinned to 0.5°x0.5°	Solar elevation Global constant	Liu et al. (2010)
OMPS (nadir)/ Suomi NNP	O ₃ partial columns	NOAA/ Eumetsat	QF>0 SOE<10° No thinning	Solar elevation Global constant	Flynn et al. (2014)
SBUV2/ NOAA-19	O ₃ partial columns	NOAA V8	QF>0 SOE<6° No thinning	Not applied	Bhartia et al. (1996), McPeters et al. (2013)
TROPOMI/ Sentinel-5P	TCO3	ESA/ DLR V1.0.0	QF>0 SOE<10° Abs(LAT)<60° Super-obbed to T511	Solar elevation Global constant	Loyola et al. (2019)

Table 1: O₃ satellite retrievals used in this paper. QF= quality flag given by data providers, SOE= Solar Elevation, LAT: Latitude, VarBC: Variational bias correction. The blacklist criteria describe when data were not used.

Instrument	NH (20-90°N)	Tropics (20°S-20°N)	SH (20-90°S)
TROPOMI (good data)	0.35±12.8	0.69±3.54	-2.83±7.42
OMI (used data)	-2.48±7.88	0.73±7.38	1.01±7.12
GOME-2A (used data)	-0.15±5.64	0.16±2.97	0.24±3.45
GOME-2B (used data)	0.35±5.8	0.24±2.82	-0.29±3.36

Table 2: Mean bias and standard deviations of the TCO3 retrievals against the CAMS ozone analysis in DU from the control experiment (CTRL).

Instrument (used data)	NH (20-90°N)	Tropics (20°S-20°N)	SH (20-90°S)
TROPOMI	0.291±6.01	0.174±2.20	-0.058±3.04
OMI	-2.74±8.06	0.51±7.36	1.21±7.04
GOME-2A	-0.267±5.73	-0.006±2.97	0.346±3.45
GOME-2B	0.287±5.86	0.083±2.88	-0.21±3.38

Table 3: Mean bias and standard deviations of the TCO3 retrievals against the CAMS ozone analysis in DU from the assimilation experiment (ASSIM).

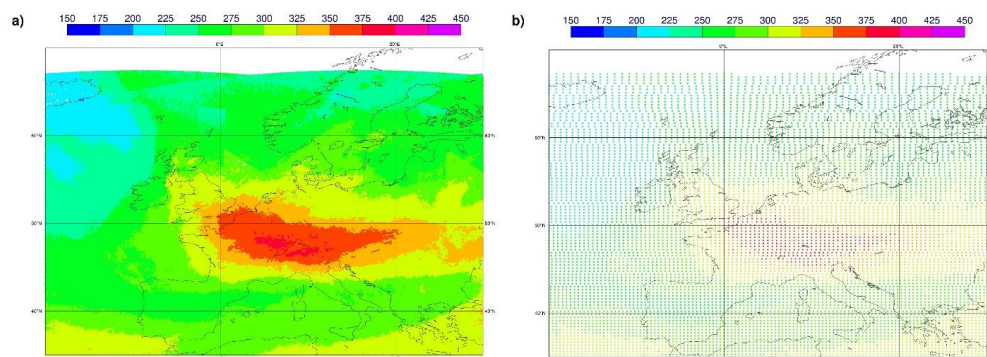
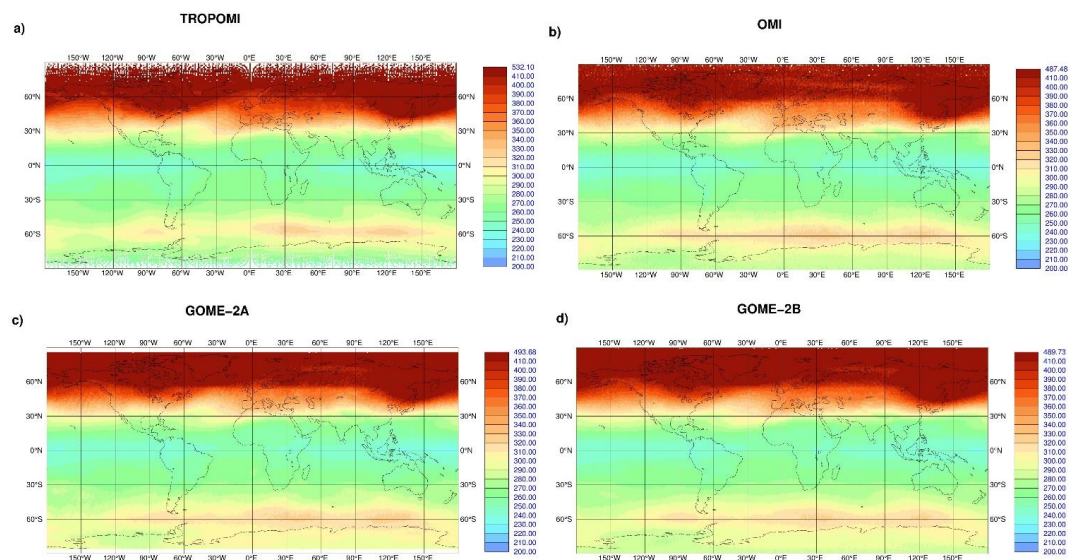


Figure 1: TROPOMI NRT TCO3 in Dobson Units (DU) at (a) full resolution and (b) super-obbed to the model resolution of T511 on 20171129, 12z over Europe.



5

Figure 2: Mean TCO3 in DU averaged over the period 26 November 2017 to 3 May 2018 from (a) TROPOMI, (b) OMI, (c) GOME-2A and (d) GOME-2B. For TROPOMI ‘good’ data are shown while for the other instruments ‘used’ data are shown.

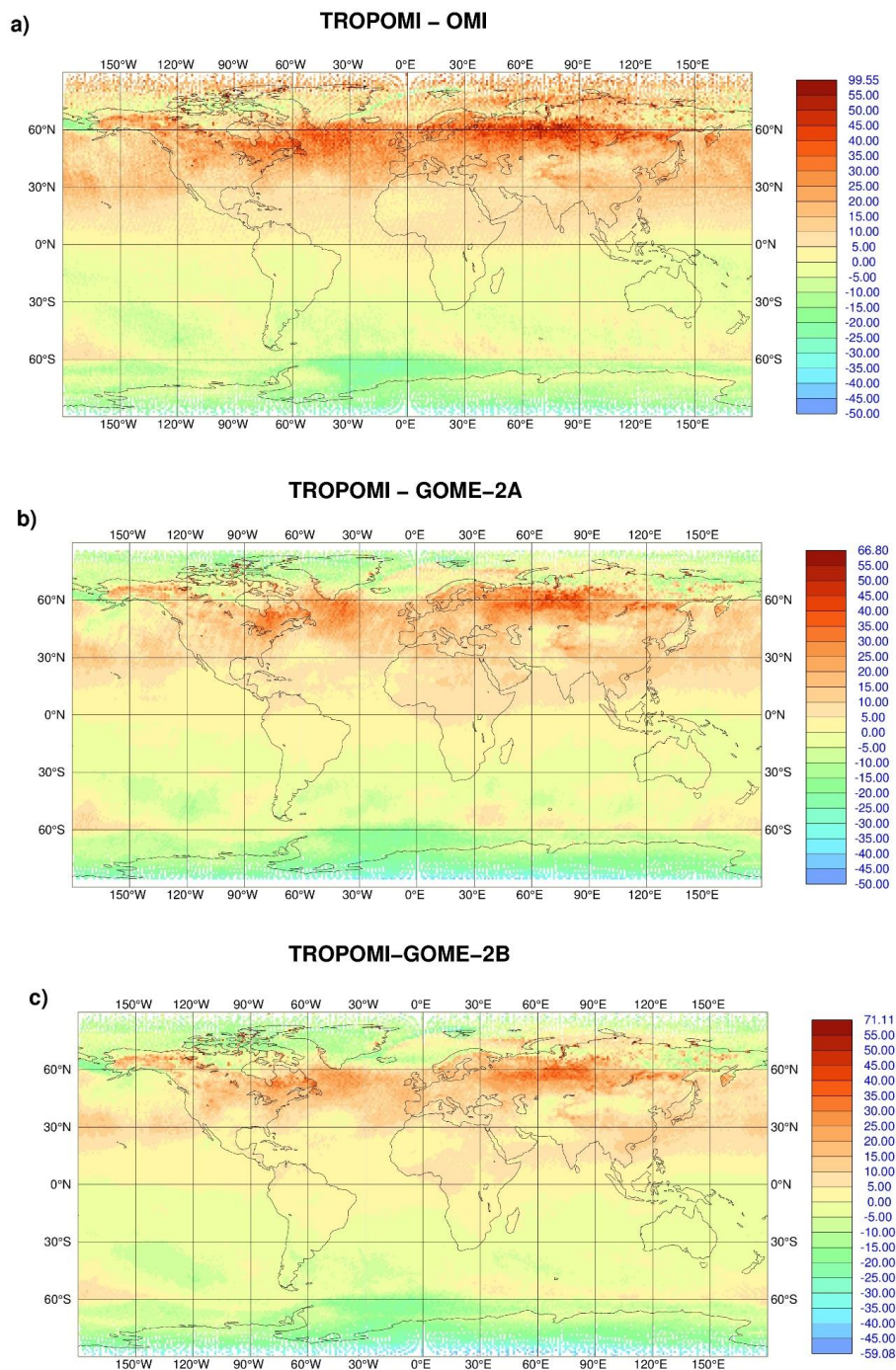


Figure 3: Mean TCO₃ differences in DU averaged over the period 26 November 2017 to 3 May 2018 from (a) TROPOMI minus OMI, (b) TROPOMI minus GOME-2A and (c) TROPOMI minus GOME-2B. Shown are ‘good’ data.

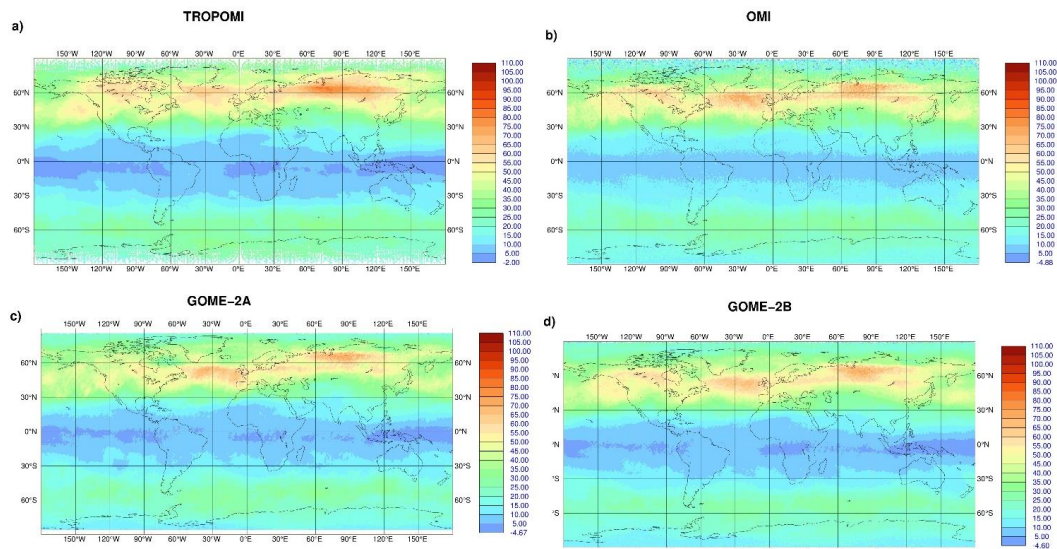
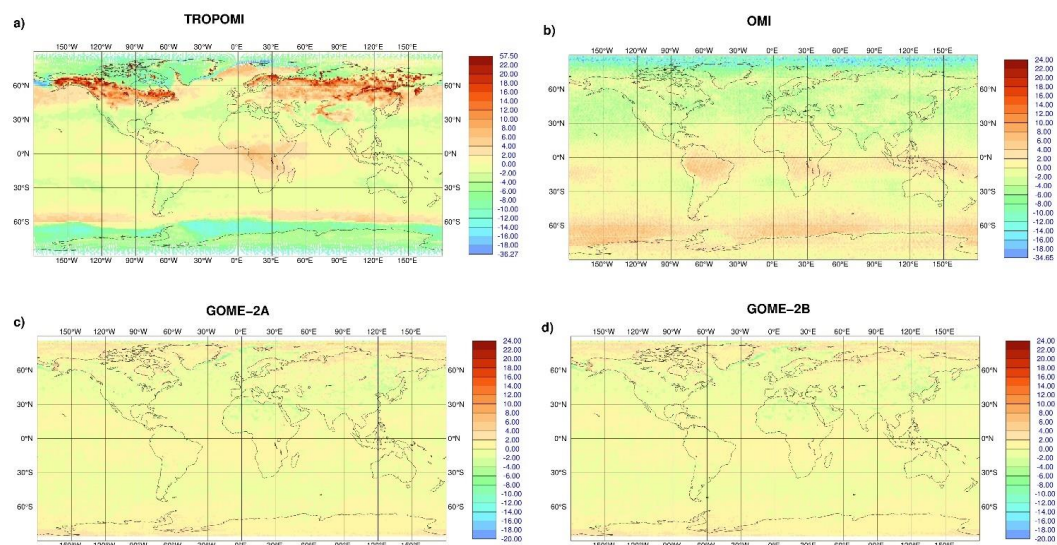
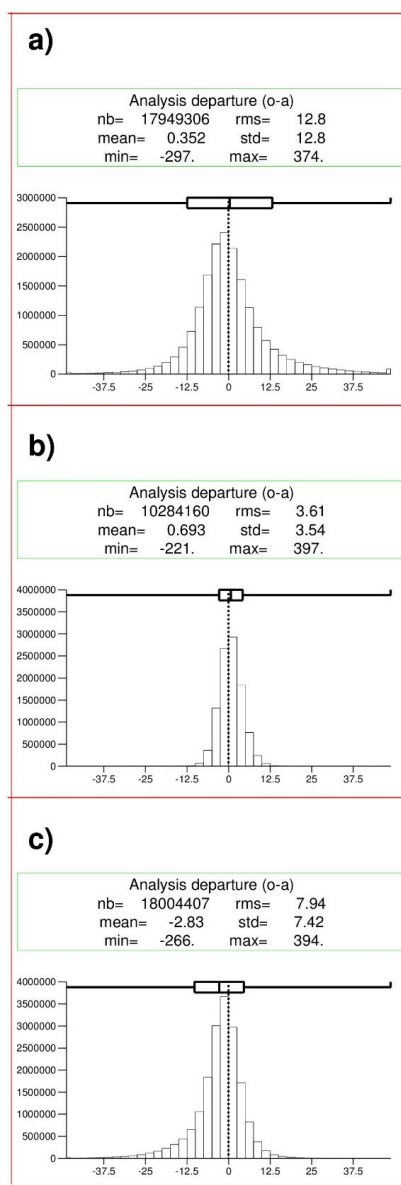


Figure 4: TCO3 standard deviation for the period 26 November 2017 to 3 May 2018 from (a) TROPOMI, (b) OMI, (c) GOME-2A and (d) GOME-2B in DU. For TROPOMI ‘good’ data are shown while for the other instruments ‘used’ data are shown.

5



10 Figure 5: Mean TCO3 analysis departures (observations minus analysis) averaged over the period 26 November 2017 to 3 May 2018 from (a) TROPOMI, (b) OMI, (c) GOME-2A and (d) GOME-2B in DU. For TROPOMI ‘good’ data are shown while for the other instruments ‘used’ data are shown.



5 **Figure 6: Histograms of TROPOMI NRT TCO₃ analysis departures for the (a) NH Extratropics, (b) Tropics and (c) SH Extratropics in DU for the period from 26 November 2017 to 3 May 2018. Shown are ‘good’ data.**

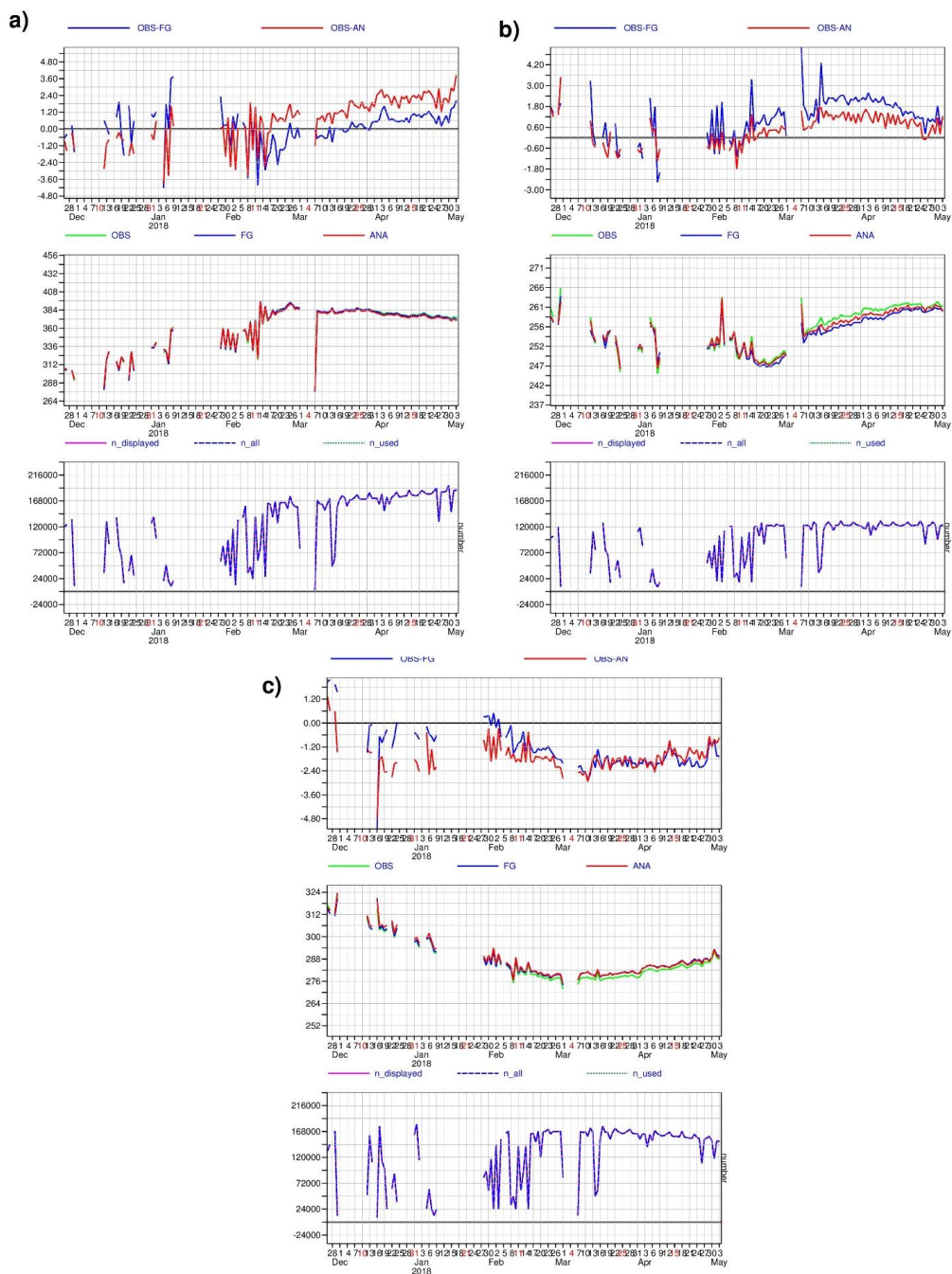


Figure 7: Time series of mean TCO3 first-guess and analysis departures (row 1), observation and analysis values (row 2) and number of data (row 3) from TROPOMI averaged over the areas (a) 70°N-20°N, (b) 20°N-20°S and (c) 20°S-70°S. Shown are 'good' data for the period 26 November 2017 to 3 May 2018. All ozone values are in DU.

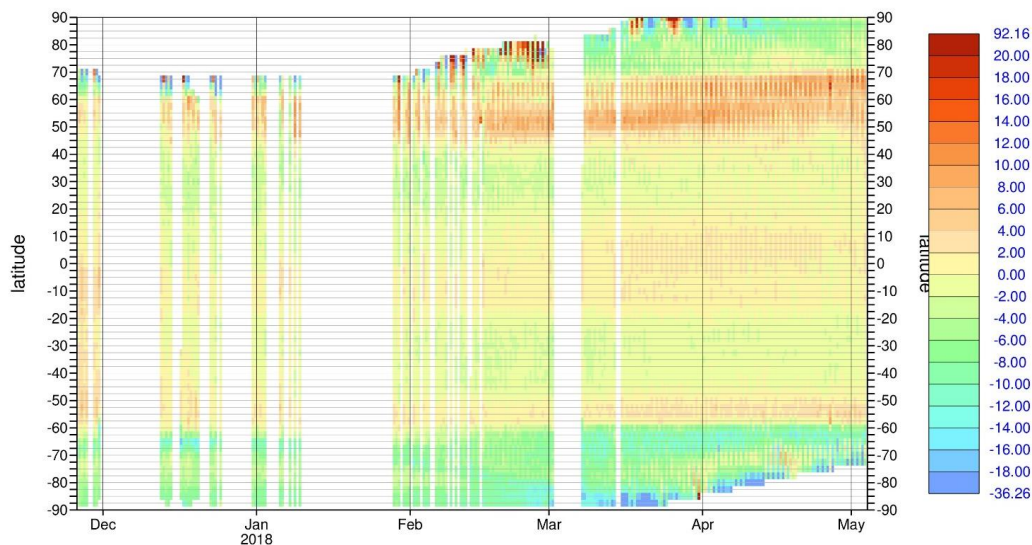
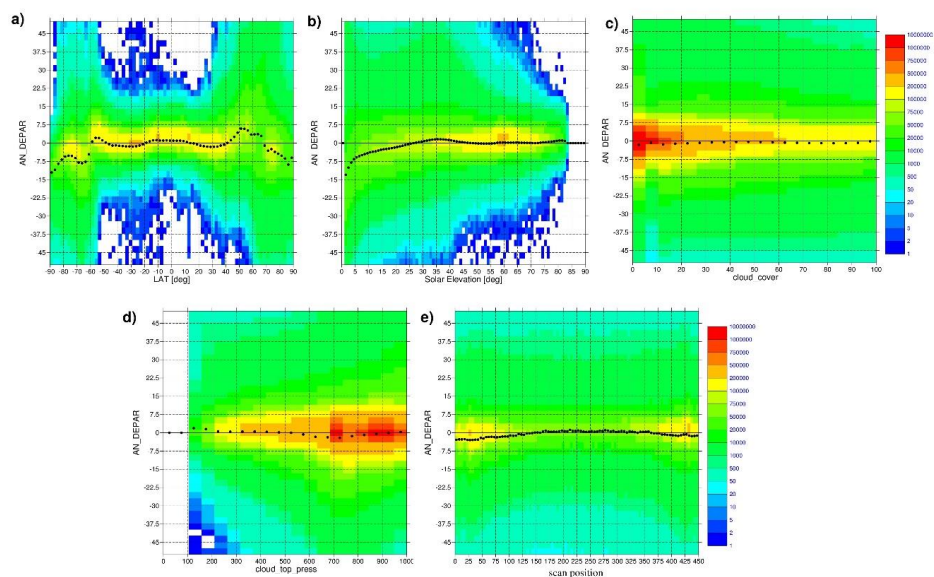


Figure 8: Timeseries of zonal mean daily analysis departures from TROPOMI NRT TCO3 in DU for the period 26 November 2017 to 3 May 2018.



5

Figure 9: Scatter plots of 'good' TROPOMI NRT TCO3 analysis departures against (a) latitude, (b) solar elevation, (c) cloud cover, (d) cloud top pressure and (e) scan position for the period 26 November 2017 to 3 May 2018. Values are in DU.

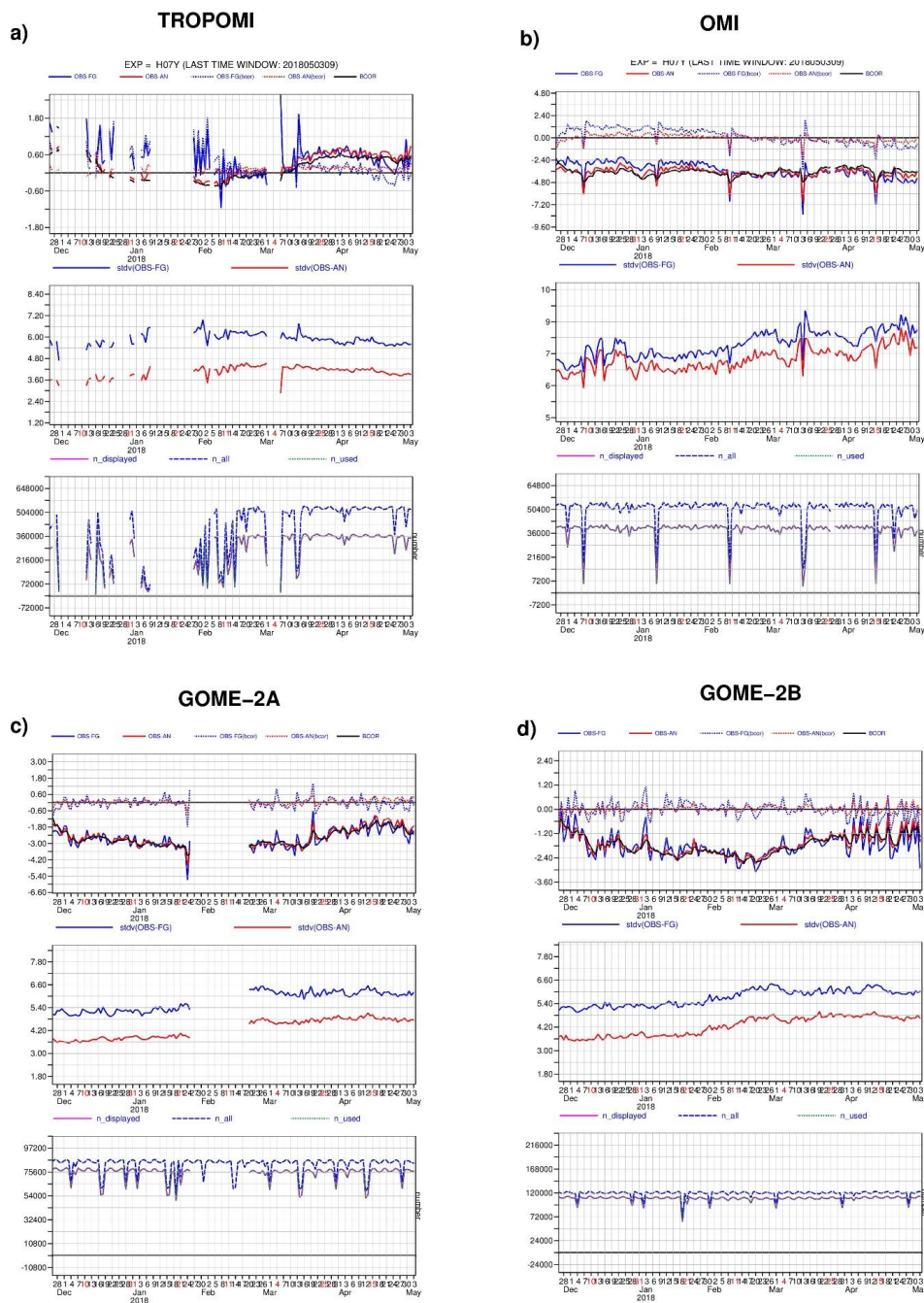


Figure 10: Time series of daily global mean TCO₃ first-guess and analysis departures (row 1), standard deviation of departures (row 2) in DU and number of data (row 3) from (a) TROPOMI, (b) OMI, (c) GOME-2A and (d) GOME-2B (bottom right) for the period 26 November 2017 to 3 May 2018. Shown are 'used' data.

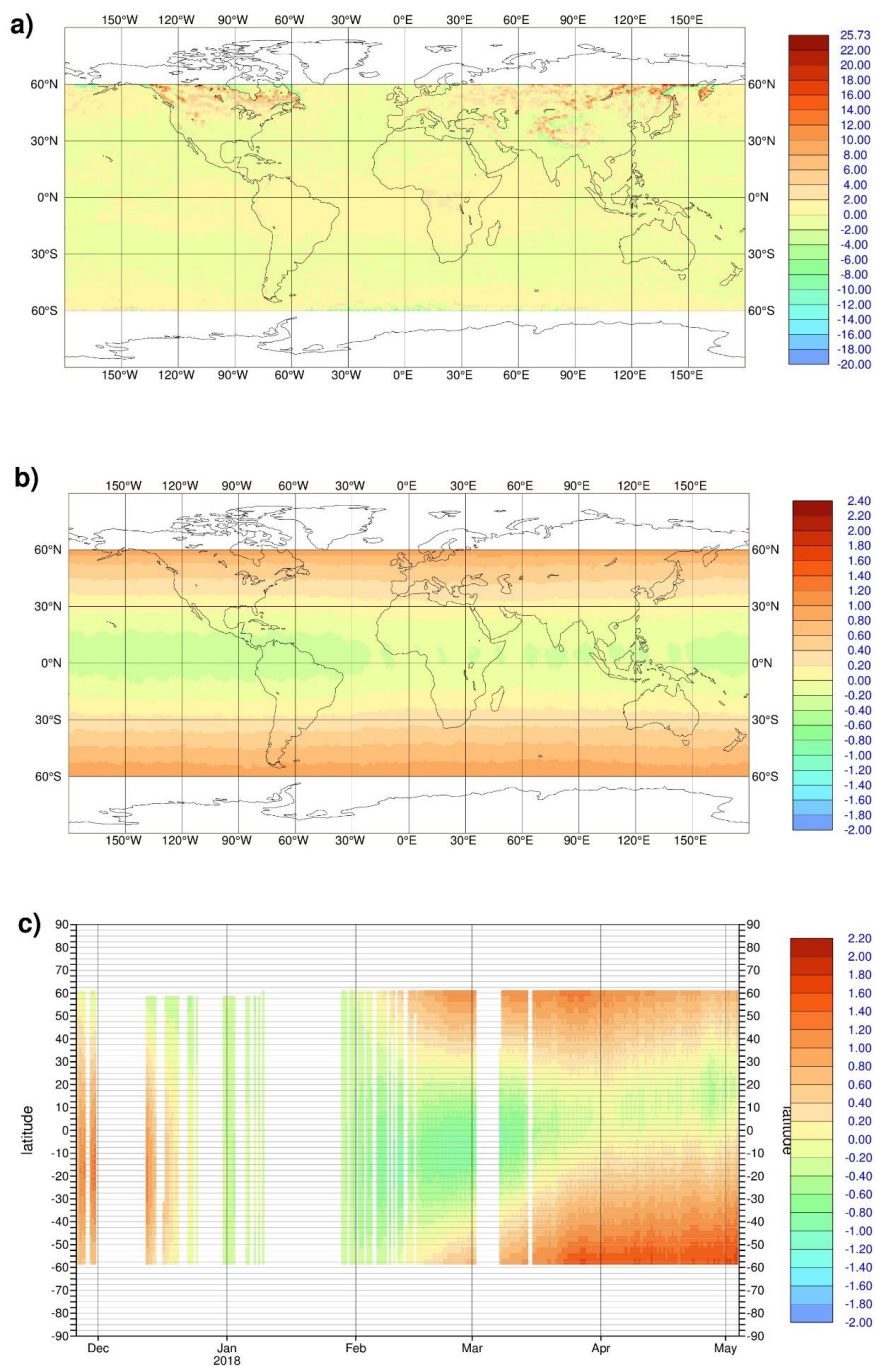


Figure 11: (a) Mean bias corrected analysis departures, (b) mean bias correction and (c) timeseries of zonal mean bias correction from TROPOMI NRT TCO3 for the period 26 November 2017 to 3 May 2018 in DU.

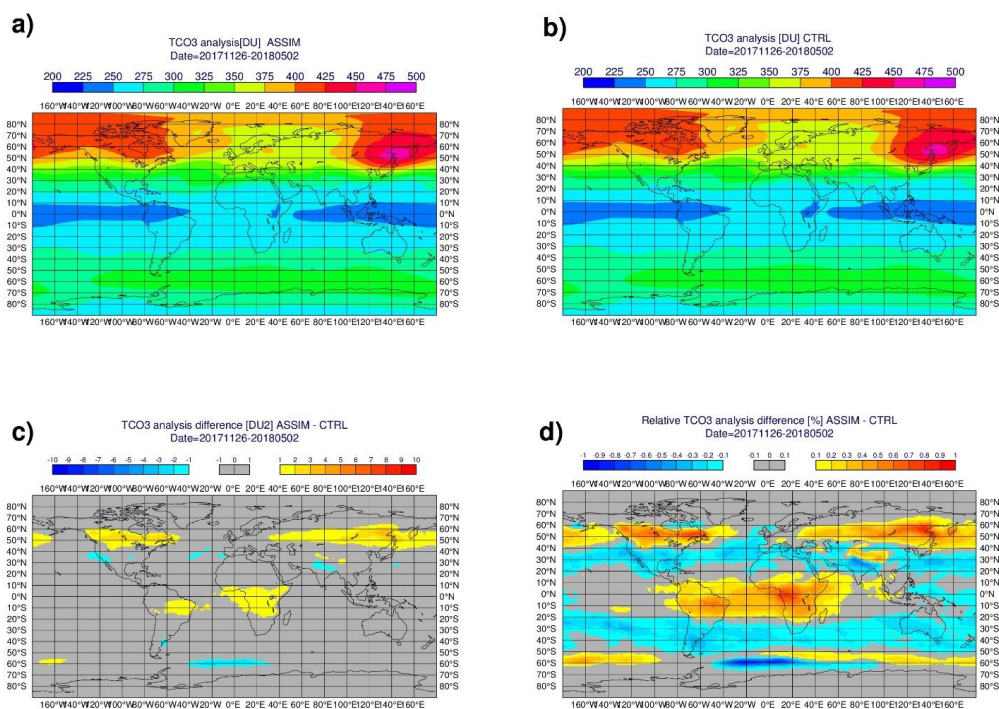


Figure 12: Mean TCO3 analysis from (a) ASSIM, (b) CTRL, as well as the (c) absolute difference in DU and (d) relative difference between ASSIM and CTRL in % for the period 26 November to 3 May 2018.

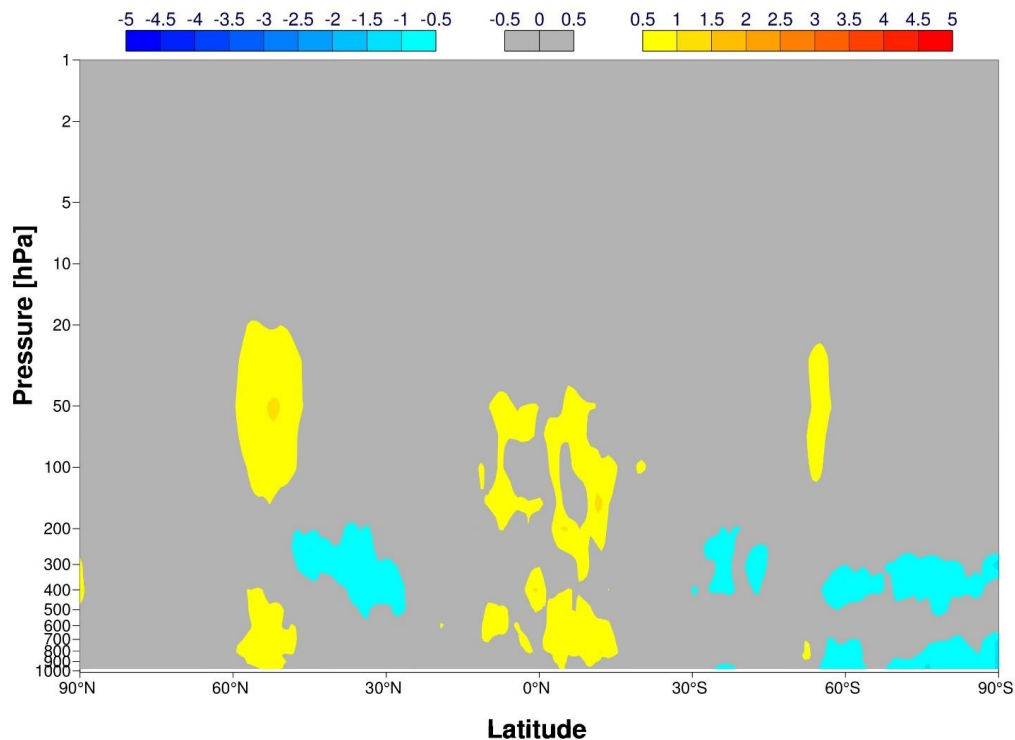
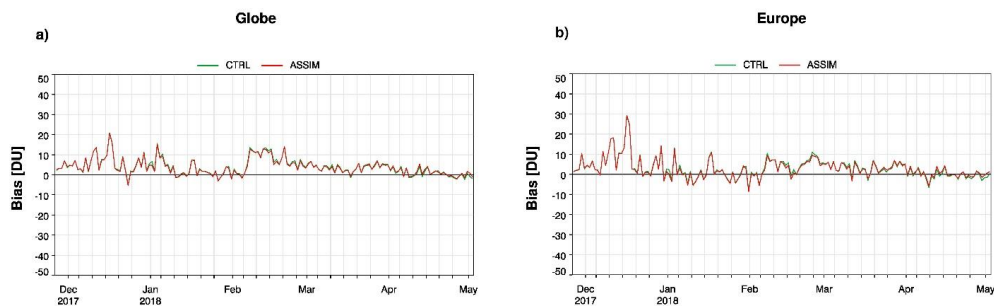


Figure 13: Cross section of relative zonal mean O_3 mixing ratio differences from ASSIM minus CTRL averaged over the period 28 January to 3 May 2018 in %.



5 Figure 14: Timeseries of daily TCO₃ bias in DU from ASSIM (red) and CTRL (blue) compared to Woudc Brewer data averaged over (a) the Globe (33 sites) and (b) Europe (20 sites).

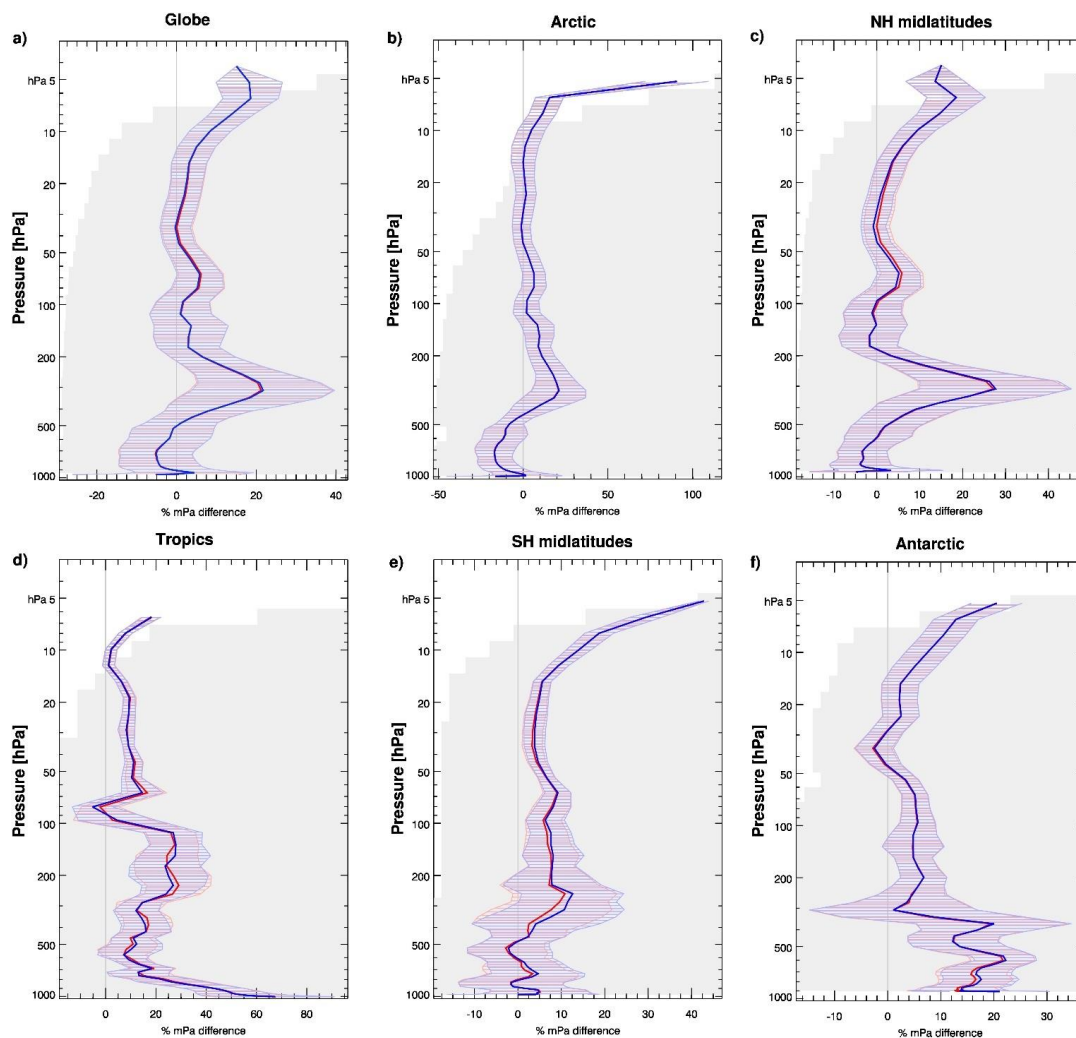


Figure 15: Mean relative O₃ bias for February to April 2018 in % between ASSIM (red) and CIRL (blue) and ozone sondes averaged over the (a) Globe, (b) Arctic, (c) NH midlatitudes, (d) Tropics, (e) SH midlatitudes and (f) Antarctic.

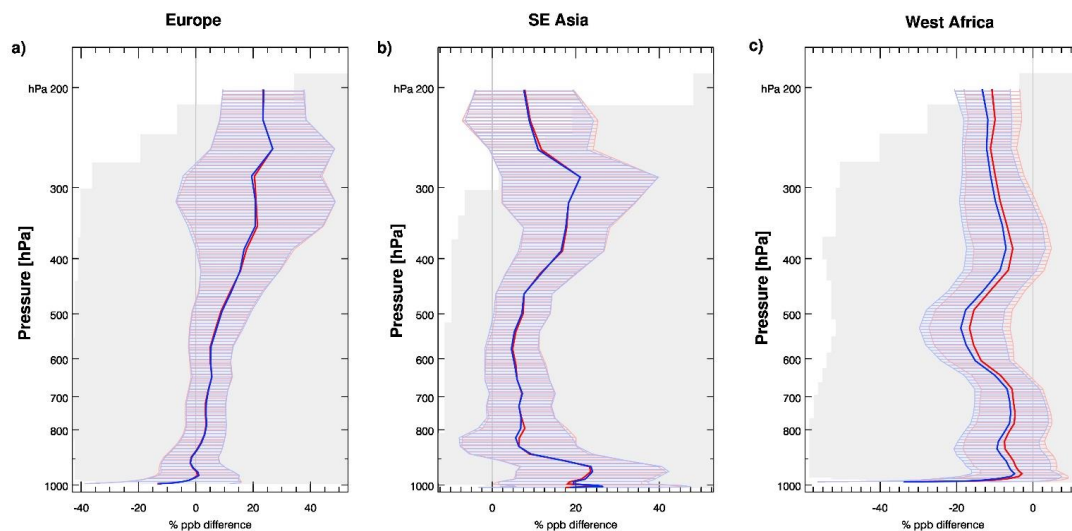


Figure 16: Mean relative O_3 difference in % of ASSIM minus IAGOS aircraft data (red) and CTRL minus IAGOS (blue) for February to April 2018 averaged over (a) European airports (13 sites, 97 profiles), (b) SE Asian airports (8 sites, 41 profiles) and (c) West African airports (14 sites, 63 profiles).

5

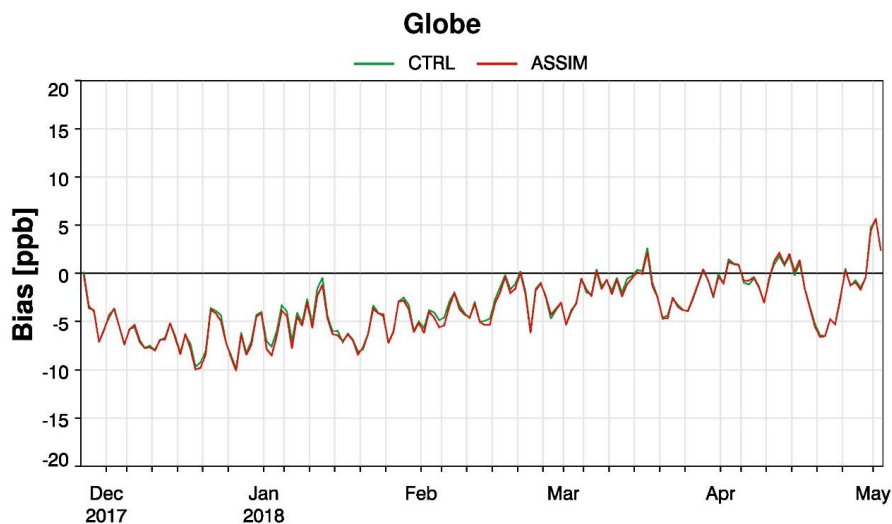


Figure 17: Timeseries of daily global mean surface O_3 bias in ppb (10 sites) from ASSIM minus GAW (red) and CTRL minus GAW (green) for the period 26 November 2017 to 3 May 2018.

10

15